

# LEDNet: Joint Low-light Enhancement and Deblurring in the Dark

— Supplementary Material —

Shangchen Zhou<sup>✉</sup>, Chongyi Li<sup>✉</sup>, and Chen Change Loy<sup>✉</sup>

S-Lab, Nanyang Technological University, Singapore  
{s200094, chongyi.li, ccloy}@ntu.edu.sg  
<https://shangchenzhou.com/projects/LEDNet>

In this supplementary material, we provide additional details and results to the paper. In Sec. **A**, we first present the architecture details of some modules in our proposed LEDNet. Sec. **B** presents further analysis and discussions on our proposed LEDNet network, consisting of more analysis and results on CurveNLU, and loss function. In Sec. **C**, we provide more analysis on our data synthesis pipeline and LOL-Blur dataset. Finally, more visual comparisons on both LOL-Blur and real-world images are provided in Sec. **D**. In addition, we present a video demo to show the effectiveness of proposed LEDNet for dealing with real-world dark blurry videos.

## A Architecture Details

As shown in Fig. 4 in the main manuscript, we adopt the existing Residual Downsample/Upsample [14] and Pyramid Pooling Module (PPM) [17] in our LEDNet. For reading convenience, Fig. 1(a) and (b) provide the detailed structures of Residual Downsample/Upsample and PPM, which are the same as their original configurations.

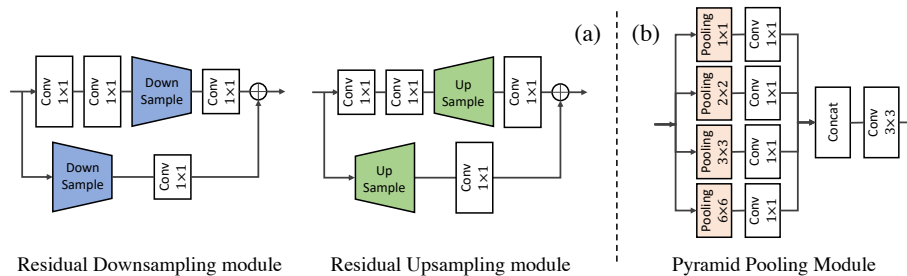


Fig. 1: Illustration of the Residual Downsample/Upsample Modules [14] and the Pyramid Pooling Module [17].

## B More Discussions on LEDNet

In this section, we first present more ablation experiments to show the effect of the key components of the proposed LEDNet, including CurveNLU, PPM, and enhancement loss.

### B.1 Analysis on CurveNLU

**Curve Parameter Visualization.** To further explore CurveNLU, we visualize an example of estimated curve parameters  $A$  in Fig. 2(a). The parameters are significantly different between unsaturated regions and saturated regions. Fig. 2(b) shows two estimated curves of blue and red points in Fig. 2(a), which lay in the unsaturated region and saturated region respectively. The red curve of the unsaturated region has the greater curvature, thus, there is a larger feature intensity increase for darker areas. In contrast, the blue curve of the saturated region that has a curvature close to 0 tends to maintain the feature value in the saturated regions. Therefore, the non-linear CurveNLU modules can increase intensity for dark areas while avoiding overexposure in the saturation regions.

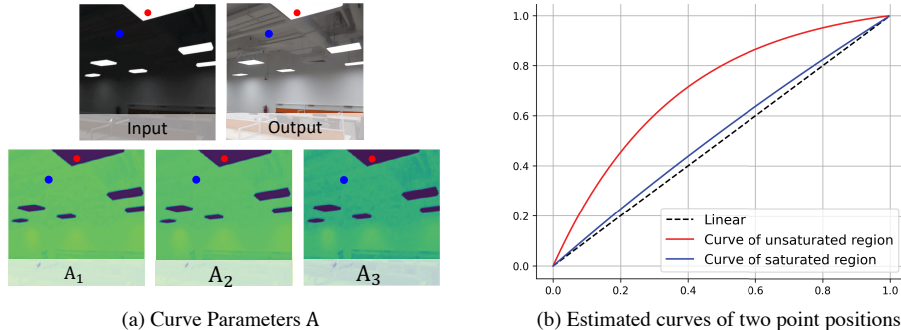


Fig. 2: (a) Visualization of estimated curve parameters. (b) Estimated curves of two points in the unsaturated region and saturated region.

**Effect of Curve Order.** To explore the effect of curve order  $n$  in the CurveNLU module, we conduct experiments that use different  $n$  for comparison. As shown in Table 1, using the higher curve order  $n$  over 3 only leads to slight PSNR/SSIM gains. Thus we use  $n = 3$  in our CurveNLU modules as a trade-off between computational complexity and performance. Notably, compared with the baseline without CurveNLU inserted, i.e.,  $n = 0$ , our proposed LEDNet obtains a large performance gain.

### B.2 Effectiveness of Enhancement Loss

Table 2 in the main manuscript has suggested that using enhancement loss  $\mathcal{L}_{en}$  is indispensable in our method. Fig. 3 further shows removing the  $\mathcal{L}_{en}$  in the train-

Table 1: Results on LOL-Blur dataset for different curve orders in CurveNLU modules.

	$n = 0$ (w/o CurveNLU)	$n = 1$	$n = 2$	$n = 3$ (Ours)	$n = 4$
PSNR	25.20	25.25	25.48	25.74	25.77
SSIM	0.823	0.826	0.838	0.850	0.850

ing process harms the visual quality significantly. The network trained without  $\mathcal{L}_{en}$  produces severe artifacts with unsmooth regions in the result.



Fig. 3: Visual comparison of different losses that using enhancement loss or not.

## C More Discussions on LOL-Blur Dataset

### C.1 Simulation of Low light

In this paper, we use the Exposure Conditioned Zero-DCE (EC-Zero-DCE) to generate the low-light images of different exposure levels. Fig. 4(a) compares our low-light data synthesis pipeline with Gamma correction that has been used in prior works [7,8]. As we can see from this comparison, the image generated by Gamma correction has a large color deviation with noticeable warm tones. In contrast, our EC-Zero-DCE can produce more natural and realistic low-light images. Moreover, the proposed EC-Zero-DCE performs pixel-wise and spatially-varying light adjustment, Fig. 4(b) provides a non-uniform luminance adjustment map for this case.

Given different exposure levels, EC-Zero-DCE can generate realistic low-light images with diverse darkness, as shown in Fig. 5. Thanks to its spatially-varying adjustment, EC-Zero-DCE tends to retain the intensities of saturated pixels, simulating the realistic light effect in real-world night images.



Fig. 4: (a) Comparisons between the proposed EC-Zero-DCE and Gamma correction for generating low-light images. (b) The non-uniform adjustment map suggests that EC-Zero-DCE performs spatially-varying luminance adjustment.



Fig. 5: The proposed EC-Zero-DCE is able to generate low-light images with different exposure levels, while keeping the intensities of saturated pixels unchanged.

## C.2 Simulation of Noise

To simulate realistic noise in dark images, we adopt CycleISP [13] to generate the noisy image in the RAW domain. We compare our noise simulation with Gaussian and Poisson noise that are commonly used in other restoration tasks, e.g., blind face restoration [5,10] and real-world blind super-resolution [11,16,1]. Fig. 6 shows the noises generated by CycleISP are more natural and realistic.

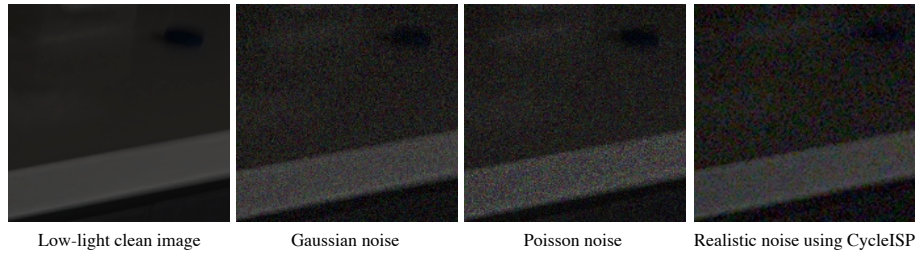


Fig. 6: Noise simulation comparison among CycleISP, Gaussian, and Poisson.

### C.3 Luminance Distribution of Datasets

Fig. 7(a) shows the luminance distribution of our proposed LOL-Blur Dataset. Fig. 7(b) provides a comparison of luminance distributions of different deblurring datasets. The great majority brightness of ground truth images in the RealBlur dataset lay the range of small intensity, thus, RealBlur is not suitable for training a light enhancement network. Besides, there are many sunny scenes in the REDS dataset, which can not be adopted to generate low-light images.

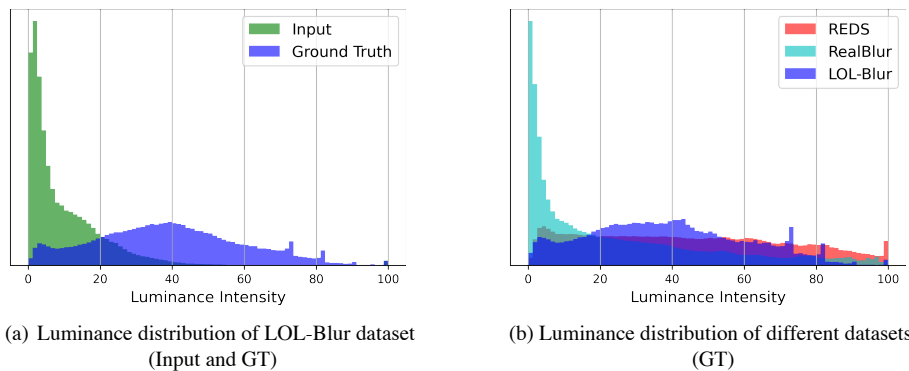


Fig. 7: (a) Luminance distribution of LOL-Blur dataset. (b) Comparison of Luminance distributions of different deblurring datasets.

## D Qualitative Comparisons

In this section, we present more visual comparisons with the baselines studied in the main manuscript: RUAS [6]  $\rightarrow$  MIMO-UNet [2], DeblurGAN-v2<sup>†</sup> [4]  $\rightarrow$  Zero-DCE [3], MIMO-UNet [2]  $\rightarrow$  Zero-DCE [3], DRBN\* [12], DeblurGAN-v2\* [4], DMPHN\* [15], and MIMO-UNet\* [2]. Fig. 8 provides more visual comparisons on our LOL-Blur Dataset. In addition, Figs. 9, 10, and 11 provide more visual comparisons on real-world night blurry images. To demonstrate the generalizability in the wild of our dataset and network, we also test on more real-world night blurry images in the RealBlur dataset [9]. Fig. 12 shows our LEDNet is able to handle various blur patterns (revealed by light streaks in the input images). Besides, Fig. 13 provides more results in different scenarios on the RealBlur dataset. The above extensive real-world results<sup>1</sup> suggest that our method performs well on diverse test images and videos in the wild.

<sup>1</sup> Note that all the Figs. 9, 10, 11, 12, and Fig. 13 provided in this suppl., as well as all results in [\[video demo\]](#) are evaluated on the real-world scenarios.

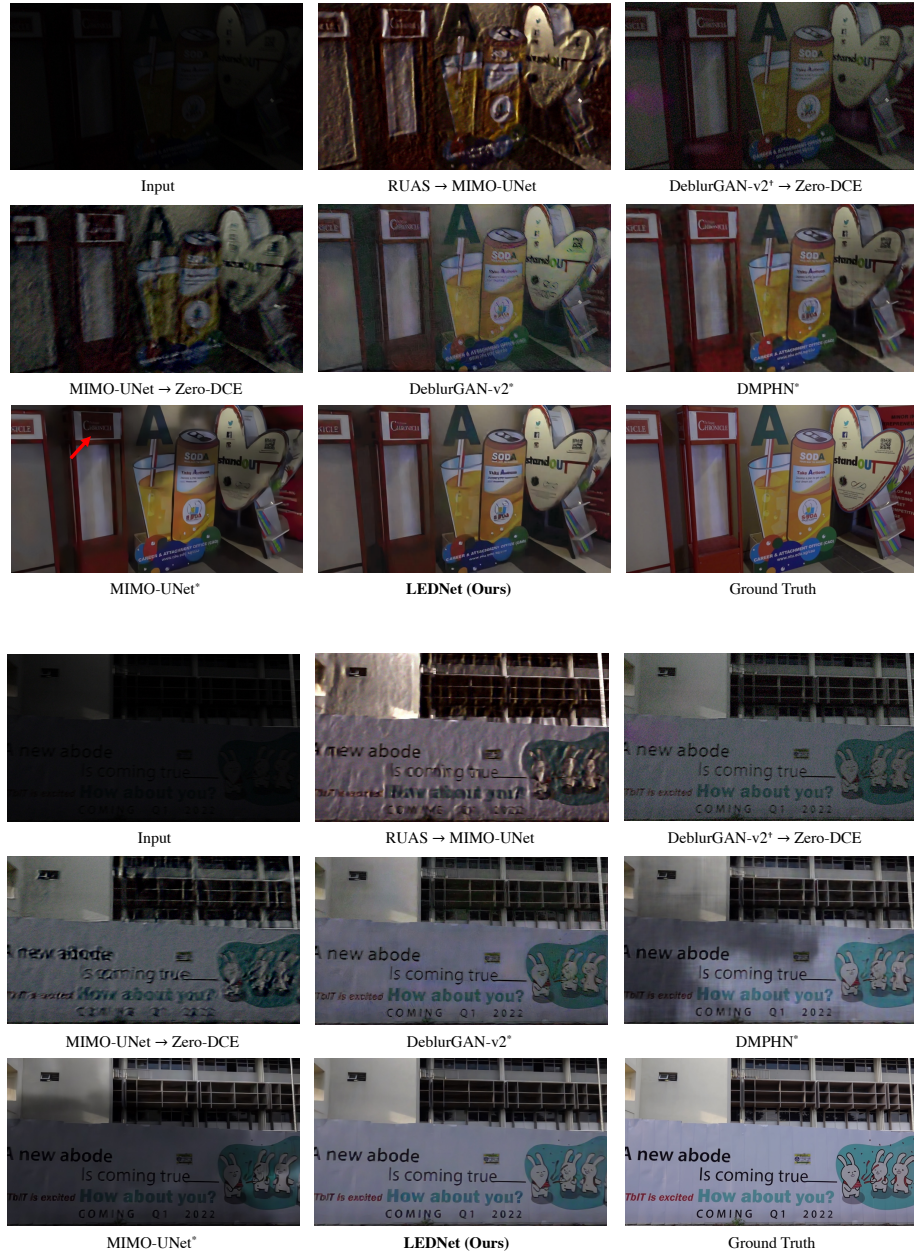


Fig. 8: Visual comparison on our LOL-Blur dataset. The proposed LEDNet generates much sharper images with visually pleasing results. The symbol ‘†’ indicates that we use DeblurGAN-v2 trained on RealBlur dataset, and ‘\*’ indicates the network is trained with our LOL-Blur dataset. **(Zoom in for best view)**



Fig. 9: Visual comparison on a real-world night blurry image. The proposed LEDNet achieves the best perceptual quality with more stable light enhancement and better deblurring performance, especially in saturated regions, while other methods still leave large blurs in saturated regions and suffer from noticeable artifacts, as indicated by red arrows. The symbol ‘†’ indicates that we use DeblurGAN-v2 trained on RealBlur dataset, and ‘\*’ indicates the network is trained with our LOL-Blur dataset. (**Zoom in for best view**)

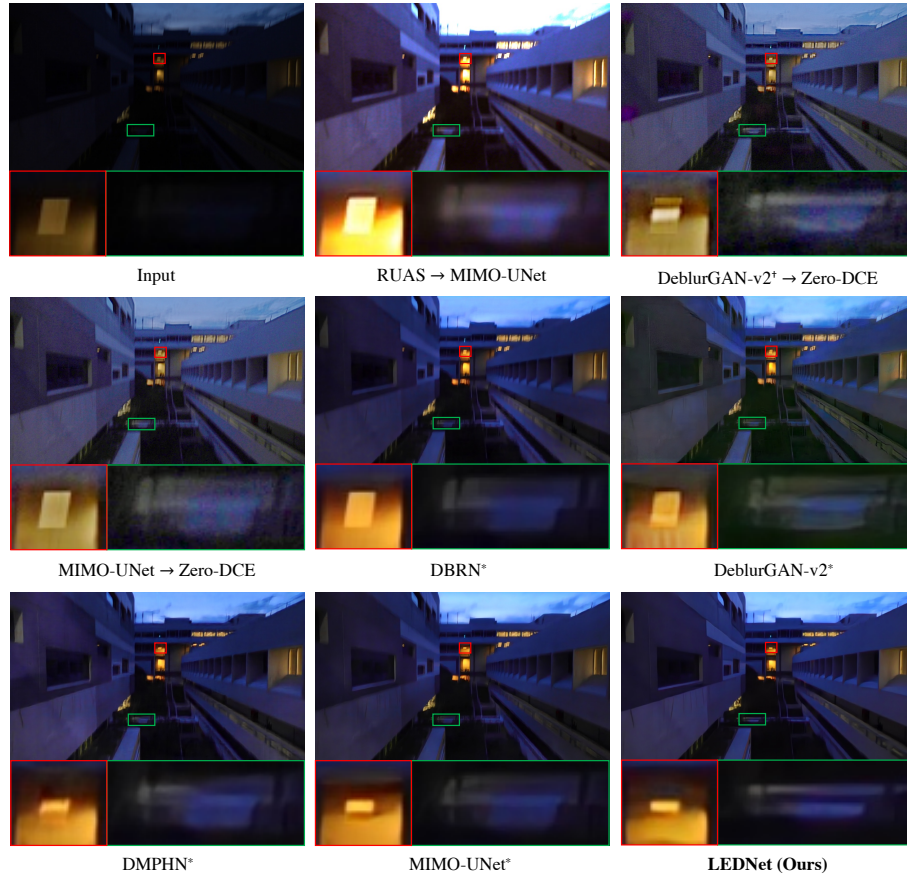


Fig. 10: Visual comparison on a real-world night blurry image. The proposed LEDNet achieves the best perceptual quality with more stable light enhancement and better deblurring performance, especially in saturated regions, while other methods still leave large blurs in saturated regions and suffer from noticeable artifacts. The symbol ‘<sup>†</sup>’ indicates that we use DeblurGAN-v2 trained on RealBlur dataset, and ‘<sup>\*</sup>’ indicates the network is trained with our LOL-Blur dataset. (**Zoom in for best view**)

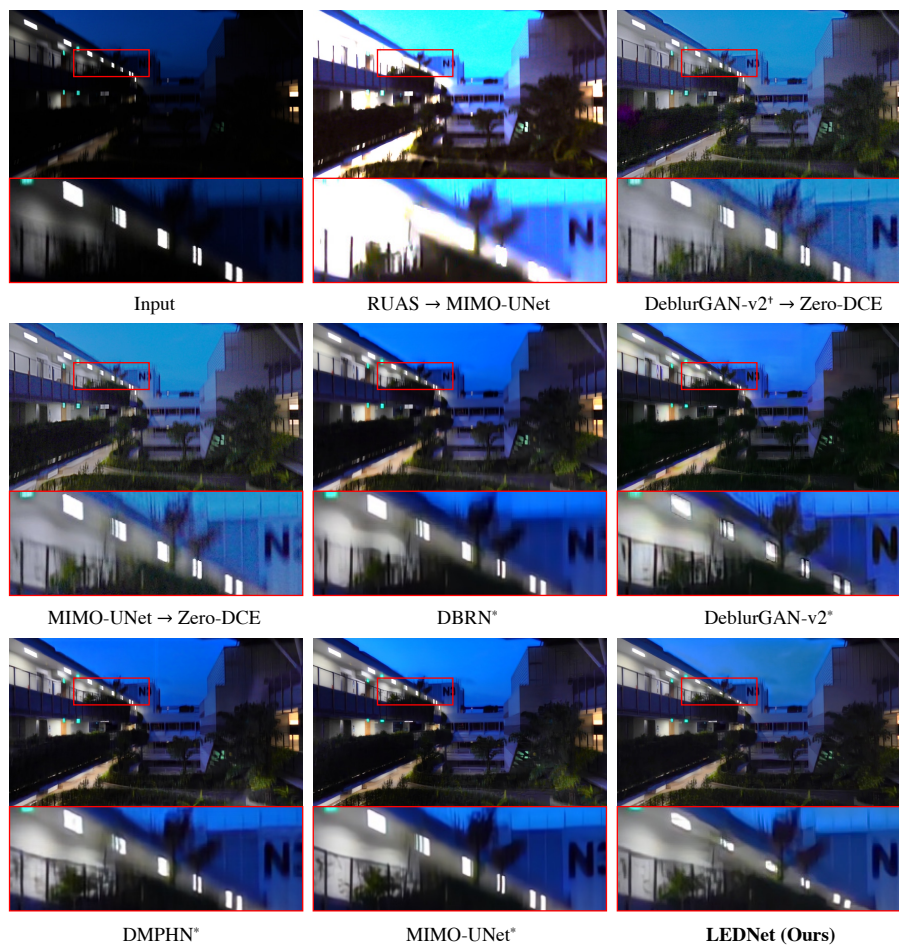


Fig. 11: Visual comparison on a real-world night blurry image. The proposed LEDNet achieves the best perceptual quality with more stable light enhancement and better deblurring performance, especially in saturated regions, while other methods still leave large blurs in saturated regions and suffer from noticeable artifacts. The symbol ‘<sup>†</sup>’ indicates that we use DeblurGAN-v2 trained on RealBlur dataset, and ‘<sup>\*</sup>’ indicates the network is trained with our LOL-Blur dataset. (**Zoom in for best view**)



Fig. 12: Evaluation on different blur patterns on RealBlur dataset [9]. The proposed LEDNet is able to handle blurs of different shapes, which can be observed from the light streaks in the input images. (Zoom in for best view)

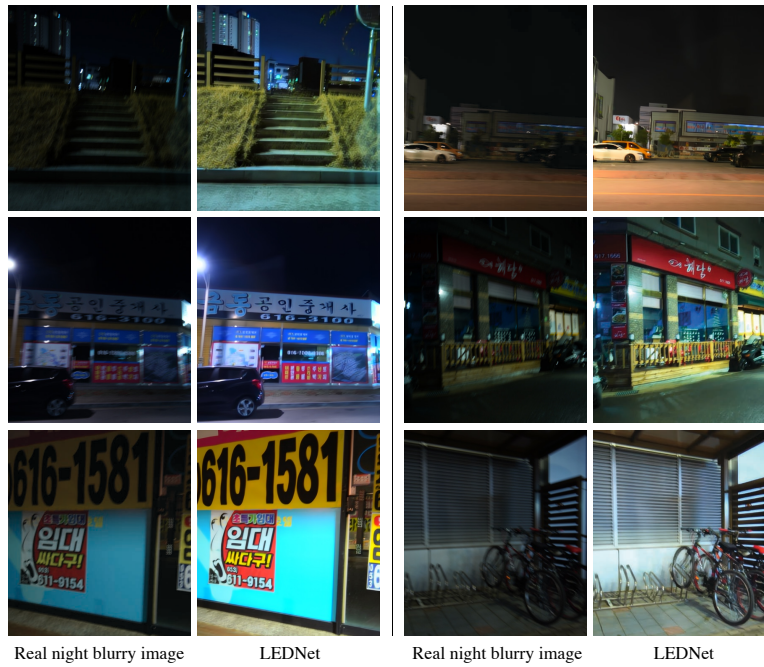


Fig. 13: Visual results on RealBlur dataset [9]. The proposed LEDNet performs well in the different scenarios. (Zoom in for best view)

## References

1. Chan, K.C., Zhou, S., Xu, X., Loy, C.C.: Investigating tradeoffs in real-world video super-resolution. In: CVPR (2022)
2. Cho, S.J., Ji, S.W., Hong, J.P., Jung, S.W., Ko, S.J.: Rethinking coarse-to-fine approach in single image deblurring. In: CVPR (2021)
3. Guo, C., Li, C., Guo, J., Loy, C.C., Hou, J., Kwong, S., Cong, R.: Zero-reference deep curve estimation for low-light image enhancement. In: CVPR (2020)
4. Kupyn, O., Martyniuk, T., Wu, J., Wang, Z.: Deblurgan-v2: Deblurring (orders-of-magnitude) faster and better. In: CVPR (2019)
5. Li, X., Chen, C., Zhou, S., Lin, X., Zuo, W., Zhang, L.: Blind face restoration via deep multi-scale component dictionaries. In: ECCV (2020)
6. Liu, R., Ma, L., Zhang, J., Fan, X., Luo, Z.: Retinex-inspired unrolling with cooperative prior architecture search for low-light image enhancement. In: CVPR (2021)
7. Lore, K.G., Akintayo, A., Sarkar, S.: Llnet: A deep autoencoder approach to natural low-light image enhancement. *Pattern Recognition* **61**, 650–662 (2017)
8. Lv, F., Lu, F., Wu, J., Lim, C.: Mbllen: Low-light image/video enhancement using cnns. In: BMVC (2018)
9. Rim, J., Lee, H., Won, J., Cho, S.: Real-world blur dataset for learning and benchmarking deblurring algorithms. In: ECCV (2020)
10. Wang, X., Li, Y., Zhang, H., Shan, Y.: Towards real-world blind face restoration with generative facial prior. In: CVPR (2021)
11. Wang, X., Xie, L., Dong, C., Shan, Y.: Real-ESRGAN: Training real-world blind super-resolution with pure synthetic data. In: ICCVW (2021)
12. Yang, W., Wang, S., Fang, Y., Wang, Y., Liu, J.: From fidelity to perceptual quality: A semi-supervised approach for low-light image enhancement. In: CVPR (2020)
13. Zamir, S.W., Arora, A., Khan, S., Hayat, M., Khan, F.S., Yang, M.H., Shao, L.: Cycleisp: Real image restoration via improved data synthesis. In: CVPR (2020)
14. Zamir, S.W., Arora, A., Khan, S., Hayat, M., Khan, F.S., Yang, M.H., Shao, L.: Learning enriched features for real image restoration and enhancement. In: ECCV (2020)
15. Zhang, H., Dai, Y., Li, H., Koniusz, P.: Deep stacked hierarchical multi-patch network for image deblurring. In: CVPR (2019)
16. Zhang, K., Liang, J., Van Gool, L., Timofte, R.: Designing a practical degradation model for deep blind image super-resolution. In: ICCV (2021)
17. Zhao, H., Shi, J., Qi, X., Wang, X., Jia, J.: Pyramid scene parsing network. In: CVPR (2017)